

Minimal Model of Prey Localization through the Lateral-Line System

Jan-Moritz P. Franosch,¹ Marion C. Sobotka,¹ Andreas Elepfandt,² and J. Leo van Hemmen¹

¹Physik Department, Technische Universität München, 85747 Garching bei München, Germany

²Institut für Biologie, Humboldt Universität, Invalidenstrasse 43, 10115 Berlin, Germany

(Received 31 December 2002; published 6 October 2003)

The clawed frog *Xenopus* is an aquatic predator catching prey at night by detecting water movements caused by its prey. We present a general method, a “minimal model” based on a minimum-variance estimator, to explain prey detection through the frog’s many lateral-line organs, even in case several of them are defunct. We show how waveform reconstruction allows *Xenopus*’ neuronal system to determine both the direction and the character of the prey and even to distinguish two simultaneous wave sources. The results can be applied to many aquatic amphibians, fish, or reptiles such as crocodilians.

DOI: 10.1103/PhysRevLett.91.158101

PACS numbers: 87.19.Bb, 05.40.–a, 87.18.–h, 87.19.La

The lateral-line system is a mechanoreceptive system of aquatic amphibians and fish. It is used to detect water movements along the animal’s body for navigation and catching prey [1–4]. It comprises, dependent on the species, some hundred to several thousand small lateral-line organs dispersed over the trunk. We analyze the clawed frog *Xenopus laevis laevis* as a typical example. Its eyes are not adapted to seeing in water and the animal’s lateral-line system has become the central sensory organ for spatial orientation [5]. *Xenopus* uses this system for catching prey in water at night. When an insect drops on the water surface, it generates a wave that passes along *Xenopus*. Depending on the waveform, the frog may or may not turn toward the wave’s origin, its prey.

Aquatic amphibians such as *Xenopus* [5] possess about 180 lateral-line organs distributed in various lines along the sides of the body around the eyes, and at a few other locations of head and neck; see Fig. 1. Reptiles such as crocodilians take advantage of about 2000 dome pressure receptors [6] on their face. Fish such as the mottled sculpin (*Cottus bairdi*) also have a lateral-line mediated prey-capture behavior [3,4], originating from several thousand receptors. In all cases the sensors are functioning in water as a medium and there are very many of them. Hence a precise temporal comparison, which needs only a few receptors as in the barn owl [7] and the sand scorpion [8], is highly improbable.

Through its lateral-line system *Xenopus* can determine direction and character of impinging waves [9]. Because each lateral-line organ responds to waves from any direction, localization requires a comparison of inputs from several lateral-line organs. *Xenopus* can also resolve the directions of two simultaneous waves of different frequency that overlap at the animal [5,10], and even discern the wave sources. Since each lateral-line organ encodes only the local superposition pattern of the waves at the body surface, this pattern-segmentation ability requires a comparison of the encoded superposition patterns from several organs and a decomposition of the patterns into their original components.

A lateral-line organ of *Xenopus* contains 4–8 small cupulae with gelatinous flags protruding into the water and being deflected by the local fluid flow [11]. The deflection stimulates sensory hair cells at the base of a cupula and in this way generates spikes in the lateral-line nerves, phase locked to the stimulus. Our simulations have shown similar results when we assumed the sensors to detect the water pressure. So the present analysis is applicable to, e.g., crocodilians [6] as well.

Stimuli such as insects scrambling at the water surface or a moving stamp in experiments [9] generate surface waves. The deflection $y_i(t)$ of cupula i at time t is proportional to the local velocity [2,11]. Here, water can be taken as a linear system [12] where the effective deflection y_i of cupula i is linear in the stimulus x^p ,

$$y_i(t) = (h_i^p \star x^p)(t) = \int_0^\infty h_i^p(\tau) x^p(t - \tau) d\tau, \quad (1)$$

where h_i^p is the so-called impulse response at cupula i while being stimulated by an impulse at position \mathbf{p} on the water surface; star \star denotes a convolution. The Fourier transform of the impulse response h_i^p is the transfer function $H_i^p(\omega) = \int h_i^p(t) \exp(-i\omega t) dt$.



FIG. 1. The clawed frog *Xenopus laevis laevis*. Its lateral-line organs can be seen clearly as white “stitches.” In the model presented here they are arranged on a circle of diameter 4 cm, a convenient but irrelevant simplification.

An approximation of the transfer function between the velocity of a moving stamp with radius $r_0 = 1.2$ cm exciting the surface of the water and the velocity at a lateral-line organ at distance $r \gg r_0$ is

$$H(\omega) = \sqrt{\frac{r_0}{r}} D_{\Delta\varphi} \exp\left[\frac{4\nu k^3}{\omega}(r_0 - r) + ik(r_0 - r)\right] \quad (2)$$

for $\omega > 0$ and $H(-\omega) = H^*(\omega)$ with ν as the water viscosity and k as the wave number. The first term on the right-hand side describes the $1/r$ reduction of the intensity due to the distance from the source [13], the second term, $D_{\Delta\varphi} = 10^{-2|\Delta\varphi|/\pi}$, accounts for the damping caused by *Xenopus*' body [14] with $\Delta\varphi$ being the angle between the direction of the lateral-line organ with respect to *Xenopus*' center and the direction of the wave source. The first term in the exponent describes amplitude reduction due to the viscosity ν [12,13] and the second term describes a phase dependence. The dispersion [12] is given by $\omega^2(k) = (gk + T_s k^3/\rho)$, where g is the gravity acceleration, T_s is the water surface tension, and ρ is the density of water.

Xenopus is able to determine the direction of a wave source. It can also distinguish sources of different frequency [15] and probably discern different preys in general. So we hypothesize *Xenopus* "tries" to determine what is going on where on the water surface. Let \mathbf{p} be a position on the water surface and let us assume *Xenopus* determines the temporal waveform of the source at \mathbf{p} . Furthermore, let $x^{\mathbf{p}}$ be the true time-dependent waveform of the source and $\hat{x}^{\mathbf{p}}$ *Xenopus*' estimate.

No known neuroanatomical data suggest or support any specific model. A minimal model is therefore our starting point, viz., answering the question of how *Xenopus* reconstructs the waveform through a minimum-variance estimator [16], i.e., by minimizing the expectation value of the least-squares error

$$\|x^{\mathbf{p}} - \hat{x}^{\mathbf{p}}\|^2 = \int_0^{T_I} [x^{\mathbf{p}}(t) - \hat{x}^{\mathbf{p}}(t)]^2 dt, \quad (3)$$

where $T_I \approx 500$ ms is the frog's minimal response time.

The only information available to *Xenopus* for determining the waveform $x^{\mathbf{p}}$ of the wave source is the spikes coming from the nerves of its lateral-line system. The spikes encode the deflection of the cupulae of the lateral-line organs. This deflection can be determined only approximately from the spike train because spike generation is a stochastic process and so is the cupula response. We model this stochasticity by adding independent Gaussian random variables $\sigma_n n_i(t)$ with mean zero and standard deviation σ_n to the deflections $y_i(t)$ of the cupulae. Moreover, each insect species generates a waveform $x^{\mathbf{p}}$ with a typical mean [13] but also with an intrinsic, stochastic, variation which is taken to be Gaussian with standard deviation σ_x .

The deflection y_i of cupula i ($1 \leq i \leq 180$) is a linear function of the wave source x given by Eq. (1) plus noise,

$$y_i = h_i^{\mathbf{p}} \star x^{\mathbf{p}} + \sigma_n n_i. \quad (4)$$

Knowing the deflections y_i of the cupulae, *Xenopus* has to "estimate" a waveform $\hat{x}^{\mathbf{p}}$ for a given waveform $x^{\mathbf{p}}$. With $\sigma := \sigma_n/\sigma_x$, the solution minimizing the error in Eq. (3) can be shown to be

$$\hat{x}^{\mathbf{p}} = \sum_j s_j^{\mathbf{p}} \star y_j, \quad S_j^{\mathbf{p}}(\omega) = \frac{H_j^{\mathbf{p}*}(\omega)}{\sum_i |H_i^{\mathbf{p}}(\omega)|^2 + \sigma^2}. \quad (5)$$

The functions $S_j^{\mathbf{p}}$ are the Fourier transforms of the reverse transfer functions $s_j^{\mathbf{p}}$, which follow from the $S_j^{\mathbf{p}}$. The transfer functions $H_i^{\mathbf{p}}$, as given by Eq. (2), depend on the position \mathbf{p} the animal is interested in.

Equation (5) shows that *Xenopus* could estimate the original waveform of the source by simply taking the convolution of deflections y_i of its lateral-line organs with built-in reverse transfer functions $s_j^{\mathbf{p}}$. The deflections y_i are represented more or less accurately in the spike trains of the lateral-line nerves. An approximate convolution can be performed efficiently and easily in neuronal hardware, as we will show below.

To get a decent approximation of the reverse transfer functions $s_i^{\mathbf{p}}$ with as few function values $s_{ik}^{\mathbf{p}}$ as possible, we choose $s_i^{\mathbf{p}}(t) \approx \sum_k s_{ik}^{\mathbf{p}} \delta(t - t_{ik}^{\mathbf{p}})$, where the $s_{ik}^{\mathbf{p}} = s_i^{\mathbf{p}}(t_{ik}^{\mathbf{p}})$ are maxima and minima of $s_i^{\mathbf{p}}$ labeled by k (inset of Fig. 2). Because the system is causal, $s_i^{\mathbf{p}}(t) = 0$ for $t > 0$. Hence $s_{ik}^{\mathbf{p}}$ with $t_{ik}^{\mathbf{p}} > 0$ do not exist.

To show explicitly that neuronal waveform reconstruction is possible, we model a neuron directly connected to the lateral-line nerves (Fig. 2), and perform the convolution of Eq. (5). Every spike in a lateral-line nerve causes a postsynaptic potential ε in the neuron. For the

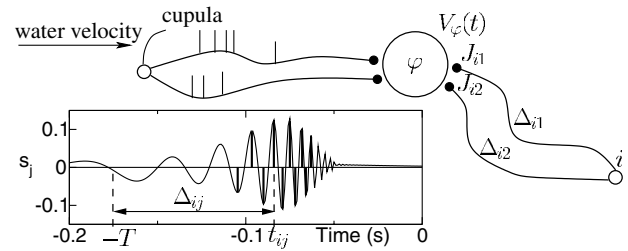


FIG. 2. Connections of a neuron, with preferred direction φ , to the lateral-line organs i (open circles). Lines denote axons, small filled circles denote synapses with strengths J_{ik} . Axonal delays Δ_{ik} and synaptic strengths are designed so that the membrane potential $V_\varphi(t)$ of the neuron approximates the original waveform $x(t)$ at the source of the water wave. Δ_{ik} and J_{ik} are provided by our model. Its localization and source-reconstruction ability needs no precise tuning of Δ_{ik} and J_{ik} . The inset shows a typical reverse transfer function s_j provided by Eq. (5) and its approximation through delta functions.

postsynaptic potential we have chosen an alpha function $\varepsilon(t) = (t/\tau) \exp(1 - t/\tau)$ for $t \geq 0$ and $\varepsilon(t) = 0$ elsewhere, with $\tau = 10$ ms. The membrane potential V^p of the neuron, modeled as a spike-response neuron [17], is

$$V^p(t) = \sum_{i,k,f} J_{ik}^p \varepsilon(t - t_i^f - \Delta_{ik}^p) + \sum_{i,k,f'} J_{ik}^{p'} \varepsilon(t - t_i^{f'} - \Delta_{ik}^{p'}),$$

where the t_i^f are the firing times of the nerve from lateral-line organ i and Δ_{ik}^p is the delay of synapse number k with synaptic strength J_{ik}^p . There are two lateral-line nerves for each lateral-line organ i , accounting for “opposite” directions of deflection [2]. One nerve spikes for deflections $y_i(t) > 0$ and so does the other one for $y_i(t) < 0$ (primed quantities f' , $J_{ik}^{p'}$, and $\Delta_{ik}^{p'}$).

One can show that the membrane potential $V^p(t)$ is approximately equal to the estimate $\hat{x}^p(t - T)$ of the waveform in Eq. (5), if we set $J_{ik}^p = s_{ik}^p$, $J_{ik}^{p'} = -s_{ik}^p$, and $\Delta_{ik}^p = T + t_{ik}^p$, explicitly demonstrating that neuronal waveform reconstruction is possible; cf. Fig. 3. Delays can be taken less than 100 ms.

We note that the synaptic efficacies J_{ik}^p and axonal delays Δ_{ik}^p depend only on the maxima and minima s_{ik}^p at times t_{ik}^p of the reverse transfer functions of Eq. (5), which in turn depend on the transfer functions of Eq. (2). As these positions are arranged on a circle, they are characterized by the direction φ . So there is a map of

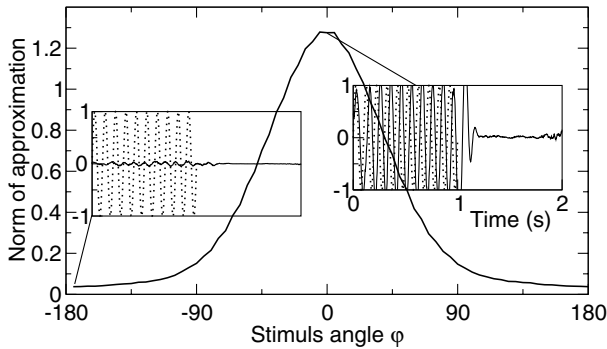


FIG. 3. A “map” of norms $\|V_\varphi\|$ of membrane potentials of 72 model neurons, each representing a different direction φ (horizontal axis). In our model, *Xenopus* swims in the direction φ where $\|V_\varphi\|$ has its maximum, which in this case is $\varphi \approx 0$. The sinusoidal wave source with frequency 10 Hz is positioned 10 cm in front of *Xenopus* ($\varphi = 0$). Each neuron reconstructs the waveform of the stimulus by means of its membrane potential $V_\varphi(t + T)$ (solid lines in the insets), “assuming” that the actual stimulus comes from direction φ . If this assumption is correct (at $\varphi = 0$), *Xenopus*’ approximation resembles the original waveform $x(t)$ (dotted lines in the insets) quite well. For wrong directions (e.g., $\varphi = 180^\circ$), *Xenopus*’ approximation is noise with a small amplitude. The present model therefore serves two purposes. First, neurons responding strongest tell *Xenopus* the direction of the wave source. Second, the membrane potential of these neurons gives *Xenopus* an approximation to the actual waveform and allows the animal to distinguish different kinds of prey.

neurons with membrane potentials $V_\varphi(t) := V^p(\varphi)$, each responsible for a certain direction φ . We assume *Xenopus* turns to the angle φ represented by the neuron that has maximal average firing rate, i.e., where the norm $\|V_\varphi\|$ as defined by Eq. (3) is maximal.

With hindsight the above assumption is reasonable because $\|V_\varphi\|$ indeed has its absolute maximum at the angle φ where the wave comes from, as shown in Fig. 3. The reason is that, when the animal is reconstructing the waveforms by Eq. (5) using a wrong direction φ , the wrong transfer functions H_j^p are used and, hence, a reconstruction gives noise only. Figure 4 shows plots of theoretical and experimental distributions of *Xenopus*’ turning angles in the lesioned and unlesioned case. To account for the results of the experiments, we have also assumed that *Xenopus* exploits no intensity but only phase information for its approximations, so that it “uses”

$$H_j^p(\omega) = \sqrt{\frac{r_0}{r_d}} \exp\left[-\frac{4\nu k^3}{\omega}(r_d - r_0) - ik(r_j^p - r_0)\right]$$

in Eq. (5) with $r_d = 10$ cm instead of the real transfer functions of water in Eq. (2); r_j^p is the distance from lateral-line organ j to position \mathbf{p} . Figure 4 indicates that these minimal assumptions already suffice to give a fair explanation of experimental reality.

For spike generation in the lateral-line nerves we have chosen an inhomogeneous Poisson process as an approximation to the real input-output characteristics [18] of the lateral-line organ. Nerve i fires in $[t, t + dt)$ with a probability of $[\pm R y_i(t) + R_s]dt$, $R = 300$ Hz, so that we get realistic spike rates lower than about 150 Hz

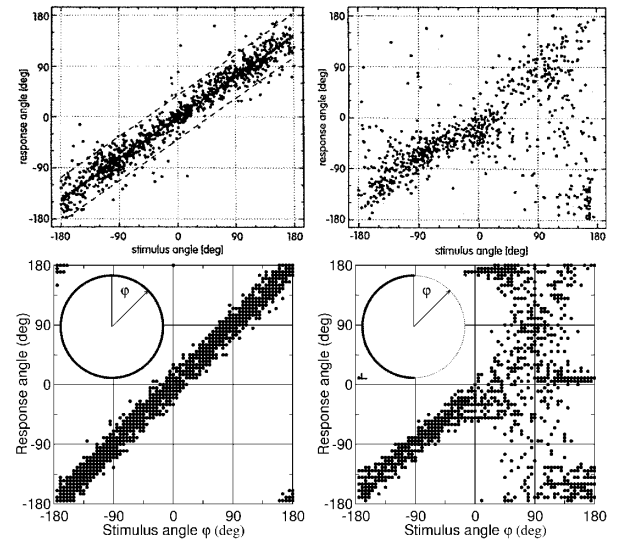


FIG. 4. Top: *Xenopus*’ experimental response angle [9] versus stimulus angle φ during 25 trials at angle $\varphi = n \times 5^\circ$, $-36 < n \leq 36$. Left: intact *Xenopus*. Right: lateral-line organs at the right-hand side have been deactivated. Bottom: Model response of neurons labeled by the φ of maximal $\|V_\varphi\|$; cf. Fig. 3. The agreement with experiment is fair.

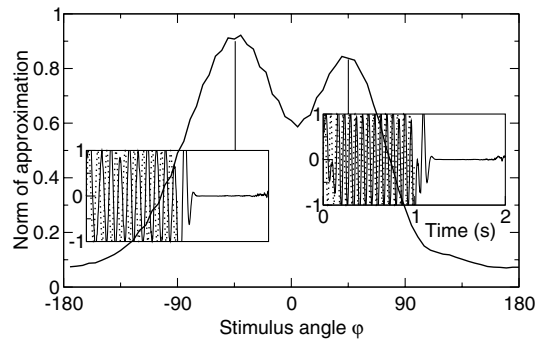


FIG. 5. “Map” like that of Fig. 3 for two simultaneous wave sources of 10 and 15 Hz, positioned at $\varphi = -45^\circ$ and 45° , 10 cm in front of *Xenopus*. The animal’s approximations are shown in the insets. In this way it could easily distinguish position and waveform of the sources, as in experiment [10].

and spontaneous rates $R_s = 10$ Hz [14]. The negative sign is for nerves that are excited by negative deflections $y_i(t) < 0$.

Two simultaneous but different wave sources can be distinguished easily by a trained *Xenopus* [10] in accordance with the present model (Fig. 5): Not only can *Xenopus* determine the positions of the two wave sources but also distinguish different frequencies. If *Xenopus* is trained to always swim to the wave source with a frequency of, say, 15 Hz with an angle between the two stimuli of, say, 90° , and the two stimuli are then presented with an arbitrary but different angle between them, *Xenopus* still turns to the 15 Hz stimulus without any further training [19]. The fact that *Xenopus* generalizes appropriately as described supports the model assumption that the actual waveform is somehow approximated by *Xenopus*.

In *Xenopus* each afferent lateral-line nerve bifurcates and then branches widely throughout the ipsilateral medullary medial octaval nucleus (MON), which is the projection nucleus of the lateral-line afferents [20]. In crocodylians neuroanatomical studies [21] indicate the very same bifurcation phenomenon. Thus a neuronal substrate might well be available for a comparison of inputs between many afferent neurons. In addition, intensive bilateral connections between the MON of both sides allow for detailed comparison between left and right side inputs [20]. As yet, recordings from neurons in the MON have not been performed because it is covered by a large blood sinus. Neurons that are sensitive to a certain direction and still show phase-locked response to the stimulus like the model neurons with membrane potential V_φ of Fig. 2 could be found here.

In summary, we have shown how a large number of sensory detectors allows an animal such as *Xenopus* to perform some kind of waveform reconstruction so as to determine both the prey’s direction and its character. A simple neuronal algorithm with realistic firing rates,

number of synapses (here 7200 per neuron), and time constants of postsynaptic potentials suffices to perform localization; see Fig. 3. Furthermore, as Fig. 4 illustrates, the model is robust in that it successfully incorporates the effect of deactivating part of the cupulae. Our theory also explains *Xenopus*’ distinguishing simultaneous wave sources, i.e., its performing pattern segmentation, as in Fig. 5. For crocodylians the question is still open, but we do not expect for long. Finally, the method of our minimal model needs minimal assumptions to allow exploring an animal’s response to sensory input efficiently, even though detailed anatomical data are not available yet—as is often the case in practice.

The authors thank Daphne Soares for her as yet unpublished alligator data. J.-M. P.F. was supported by the Graduate School “Sensory Interactions” (GRK 267).

- [1] G. Kramer, *Zool. Jb. Physiol.* **52**, 629 (1933).
- [2] I. J. Russell, in *Frog Neurobiology: A Handbook*, edited by R. Llinas and W. Precht (Springer, Berlin, 1976), pp. 513–550.
- [3] *The Mechanosensory Lateral-Line: Neurobiology and Evolution*, edited by S. Coombs, P. Görner, and H. Münz (Springer, New York, 1989).
- [4] S. Coombs, J. J. Finneran, and R. A. Conley, *Philos. Trans. R. Soc. London, Ser. B* **355**, 1111 (2000).
- [5] *The Biology of Xenopus*, edited by R. C. Tinsley and H. R. Kobel (Oxford University Press, Oxford, U.K., 1996).
- [6] D. Soares, *Nature (London)* **417**, 241 (2002).
- [7] C. E. Carr, *Annu. Rev. Neurosci.* **16**, 223 (1993).
- [8] W. Stürzl, R. Kempster, and J. L. van Hemmen, *Phys. Rev. Lett.* **84**, 5668 (2000).
- [9] B. Claas and H. Münz, *J. Comp. Physiol.* **178**, 253 (1996).
- [10] A. Elepfandt, *Neurosci. Lett. (Suppl.)* **26**, 380 (1986).
- [11] A. J. Kalmijn, in *Sensory Biology of Aquatic Animals*, edited by J. Atema, R. R. Fay, A. N. Popper, and W. N. Tavolga (Springer, New York, 1988), pp. 83–130.
- [12] H. Lamb, *Hydrodynamics* (Cambridge University Press, Cambridge, U.K., 1932), 6th ed., Sects. 226ff, 246, 331f.
- [13] H. Bleckmann, *Reception of Hydrodynamic Stimuli in Aquatic and Semiaquatic Animals* (Fischer, Stuttgart, 1994).
- [14] A. Elepfandt and L. Wiedemer, *J. Comp. Physiol. A* **160**, 667 (1987).
- [15] A. Elepfandt, B. Seiler, and B. Aicher, *J. Comp. Physiol. A* **157**, 255 (1985).
- [16] B. L. van der Waerden, *Mathematical Statistics* (Springer, Berlin, 1969).
- [17] W. Gerstner and J. L. van Hemmen, in *Models of Neural Networks II*, edited by E. Domany, J. L. van Hemmen, and K. Schulten (Springer, New York, 1994), pp. 39–47.
- [18] D. Strelhoff and V. Honrubia, *J. Neurophysiol.* **41**, 432 (1978).
- [19] K. Schroedter, Staatsexamensarbeit, Humboldt Universität zu Berlin, 2002 (unpublished).
- [20] W. Plassmann, *J. Comp. Physiol.* **136**, 203 (1980).
- [21] D. Soares (private communication).